

# Methods for Manufacture of Corrugated Wire Mesh Laminates

Jeongho Choi, Krishna Shankar, Alan Fien, and Andrew Neely

**Abstract**— Corrugated wire mesh laminates (CWML) are a class of engineered open cell structures that have potential for applications in many areas including aerospace and biomedical engineering. Two different methods of fabricating corrugated wire mesh laminates from stainless steel, one using a high temperature Lithobraz alloy and the other using a low temperature Eutectic solder for joining the corrugated wire meshes are described herein. Their implementation is demonstrated by manufacturing CWML samples of 304 and 316 stainless steel (SST). It is seen that due to the facility of employing wire meshes of different densities and wire diameters, it is possible to create CWML laminates with a wide range of effective densities. The fabricated laminates are tested under uniaxial compression. The variation of the compressive yield strength with relative density of the CWML is compared to the theory developed by Gibson and Ashby for open cell structures [22]. It is shown that the compressive strength of the corrugated wire mesh laminates can be described using the same equations by using an appropriate value for the linear coefficient in the Gibson-Ashby model.

**Keywords**— cellular solids, corrugation, foam, open-cell, metal mesh, laminate, stainless steel

## I. INTRODUCTION

WHEN planning the manufacture of a new product, one of the main concerns of the relevant industries is the cost effectiveness of the product. Engineering research considers economical manufacturing to be the most important objective. In this case cost effectiveness as well as the length of manufacturing time to make the new product, the difficulty in setting up appropriate manufacturing systems for its production, and applications of the new product have to be considered. A number of these factors are governed by the fabrication system employed. This paper describes investigation and development of methods of fabricating Corrugated Wire Mesh Laminates (CWML) in a cost effective manner. CWML are open celled structures with a regular

Jeongho Choi is with the University of New South Wales of school of aerospace, civil, and mechanical engineering, Canberra, ACT 2600 Australia (corresponding author to provide phone: 61-2-6268-8593; fax: 61-2-6268-8276; e-mail: JeongHo.choi@student.adfa.edu.au).

Krishna Shankar is with the University of New South Wales of School of Aerospace, Civil, and Mechanical Engineering, Canberra, ACT 2600 Australia. (e-mail: k.shankar@adfa.edu.au).

Alan Fien is with the University of New South Wales of School of Aerospace, Civil, and Mechanical Engineering, Canberra, ACT 2600 Australia. (e-mail: a.fien@adfa.edu.au).

Andrew Neely is with the University of New South Wales of School of Aerospace, Civil, and Mechanical Engineering, Canberra, ACT 2600 Australia. (e-mail: a.neely@adfa.edu.au).

geometric configuration and relatively high relative densities that can be tailored by the selection of the mesh and corrugation properties. They have many potential applications including use in heat exchanger units, as core material for sandwich constructions, and as bone replacement material in biomedical implants. In this paper, a solder paste-bonding system is proposed for making CWML products by using vacuum or an inert gas environment.

Vacuum solder bonding techniques have been investigated and well established by many previous advanced technological investigations. Their main advantage is their capacity for protection from oxidation. Solder bonding of metallic materials requires relatively high temperatures. At these elevated temperatures, the presence of oxygen in the atmosphere presents a severe problem. Oxidation of the specimen surface and the solder material severely affects their bonding capabilities and results in joints with poor bond strength as well as specimens with corrosion damage. Hence it is required to employ a manufacturing system which ensures that oxygen is kept out of the environment during the soldering process. Protection from oxidation can be provided by the use of an inert gas environment, the use of flux material or by conducting the manufacturing in a vacuum furnace. A common method for shielding from oxygen is the use of an inert Argon gas environment. H. Lee et al. [1] focused on the solid-state diffusion bonding within an inert gas environment. Vacuum, inert gas, or fluxes are common environments used for brazing bonding procedure in industries [2]. A constant supply of Argon gas into the furnace keeps atmospheric oxygen away and improves bonding performance [3-6]. Another method of oxygen protection is vacuum environment. Kim et al. designed and constructed an ultra-high vacuum diffusion-bonding device, for joining different metal interfaces [7]. Eroglu et al [8] carried out diffusion bonding out of Titanium alloy with stainless steel with a copper interlayer in vacuum at elevated temperatures using applied pressure. To ensure good bonding of the joints in the specimen, the vacuum environment has to be applied along with appropriate levels of temperature, and pressure for the duration of the bonding process. To bond components of same or similar type material, liquid phase joining is normally employed. This involves using a bonding material that becomes liquid at relatively low temperatures which then works its way into the joints to bond the materials. Charles L. Bauer [9] suggested the use of liquid phase bonding for joining different metals and alloys, consisting of soldering and brazing. Lugscheider et al [10] recommends the use of Transient Liquid Phase (TLP) bonding which is based on the principle that isothermal solidification happen after diffusion of a high melting material, low melting material, and intermetallic

phases. According to [11] the TLP process produces a strong interface free joint with no remnant of bonding agent. By placing a thin interlayer of alloying metal containing a melting point depressant between two pieces of parent material and heating the entire assembly, a liquid interlayer is formed. The liquid then fills voids formed by unevenness of the mating surfaces. TLP differs from diffusion bonding in that the formation of a thin liquid interlayer eliminates the need for high clamping force [11]. For the bonding of Titanium alloys for use in biomedical applications, Molybdenum (Mo) and Tin (Sn) are recommended as safer elements for the living body [12]. Lugscheider et al [13] states that transient liquid phase (TLP) bonding processes are novel, trend-setting technologies in the field of joining dissimilar materials, and that these have been specifically adapted to the requirements of the microsystems. In particular, eutectic Tin-Silver (Sn-Ag) alloy is one of the promising candidates for surface mounting technology for the next generation [14].

Fabrication of advanced cellular solid structures using metallic elements has been investigated by many researchers in the last two decades. The use of crimped wire mesh was first explored by Chisholm [15], who manufactured a crimped wire mesh heat exchanger. Sypeck et al. [16] invented manufacturing processes for metallic cellular solids based on foam, lattice, and multi-functional designs with different materials. The structures they created had open, closed and mixed types of porosity, in which the cell types were uniformly arranged in controlled, three-dimensional space-filling arrays. The bonding methods employed involved solid-state, liquid-phase, and other technologies [17].

In the current work, two different methods of manufacturing corrugated wire mesh laminates, are presented. Both are based on employing solder bonding technique within an inert Argon gas environment. One technique uses the Lithobraz 925 silver based cadmium free filler metal as the bonding agent while the other uses a liquid Tin based eutectic solder (95Sn-5Ag). The Lithobraz soldering is performed at an elevated temperature of 925<sup>o</sup>C, while the Sn-Ag Eutectic soldering is conducted at a significantly lower temperature, 225<sup>o</sup>C. Due to the higher temperatures required for the Lithobraz soldering, protection from oxidation necessitated a more complex set up, while the low temperature Eutectic soldering could be accomplished in a much simpler set up. The relative densities of CWML laminates manufactured by these methods are assessed by comparison with the open-cell model by Gibson-Ashby.

TABLE I  
 DETAILS OF STEEL MESH

Sample Designation	Mesh per		Wire diameter		Opening width		Density of mesh $\rho^*/\rho_s$	
	inch	mm	inch	mm	inch	mm		
304SST	A	24	0.945	0.0140	0.356	0.0280	0.7112	0.262
	B	26	1.024	0.0075	0.191	0.0318	0.8084	0.150
	C	26	1.024	0.0075	0.191	0.0310	0.7874	0.153
	D	28	1.102	0.0100	0.254	0.0260	0.6604	0.218
	E	32	1.260	0.0065	0.165	0.0250	0.6350	0.162
	F	40	1.575	0.0095	0.241	0.0160	0.4064	0.293
	G	50	1.969	0.0090	0.229	0.0110	0.2794	0.353
	H	80	3.150	0.0070	0.178	0.0060	0.1524	0.423
316SST	K	27	1.063	0.00866	0.22	0.03740	0.95	0.148

## II. METHODOLOGY

### A. Materials

Wire meshes of two types of AISI stainless steel (SST) were employed in the study: 304SST and 316SST. While these two types of steel have different chemical compositions, they have the same mechanical properties in terms of Young's modulus [193 GPa] and Yield strength [205 MPa] and a density of 8.0 g/cm<sup>3</sup>. The chemical composition of type 304SST is 0.08% C, 17.5-20% Cr, 8-11% Ni, <2% Mn, <1% Si, <0.045% P, <0.03% S. In addition to the above alloying elements, 316SST as also has P, Mo, and N. The chemical composition of type 316SST is 0.03% C, 16-18.5% Cr, 10-14% Ni, 2-3% Mo, <2% Mn, <1% Si, <0.045% P, <0.03% S, <0.1% N. According to the American Society of Testing Materials (ASTM D-2651-01), type 316SST has a much greater corrosion resistance because of the presence of Mo in it.

The CWML laminate is fabricated with corrugated cylindrical woven wire metal mesh [18]. The Lithobraz soldering technique was employed to fabricate eight samples of CWML each with a different grade of 304SST wire mesh. Different grades of wire meshes have different mesh densities and/or wire diameters. The low temperature Eutectic soldering technique was employed to manufacture 16 CWML laminates, but all of them using the same grade of 316SST wire mesh. Table I shows details of wire mesh grades employed for both the fabrication methods. The mesh density (number of wires per unit area) is listed in the second pair of columns in terms of mesh per inch and mesh per millimeter (mm) and the wire diameter and opening widths are listed in the third and fourth pairs of columns. The last column lists the relative density of the wire meshes used for the manufacture as  $\rho^*/\rho_s$ , where  $\rho^*$  is the effective density of the mesh, while  $\rho_s$  is the density of the wire material (304SST or 316SST). In general the relative density increases with increasing mesh per inch (number of wires per inch), however it also depends on the diameter of the wire. The relative densities of the 304SST meshes ranged from 0.150 to 0.423 while the relative density of the 316SST mesh used was 0.148.

### B. Fabrication of CWML by Lithobraz Technique

The brazing material employed for this fabrication method was Lithobraz 925. Lithobraz 925 consists of 92.5Ag-7.3Cu-0.2Li by wt.% and, due to its 0.2% Lithium content, has a melting temperature upwards of 760<sup>o</sup>C (1400<sup>o</sup>F), and liquidus at 890<sup>o</sup>C (1635<sup>o</sup>F). The recommended minimum brazing temperature is 900<sup>o</sup>C (1652<sup>o</sup>F), and maximum operating temperature 260<sup>o</sup>C (500<sup>o</sup>F) [19].

The Lithobraz fabrication was conducted at 925<sup>o</sup>C in an inert Argon gas environment. As mentioned before, because of the high brazing temperature, a specially designed box had to be used inside the furnace in order to ensure complete elimination of atmospheric oxygen. Fig.1 shows schematic diagrams of the CWML laminate on the left and the fabrication box assembly on the right [20]. Note that the CWML laminate is constructed with cross ply corrugated wire mesh layers, i.e.

with the direction of the corrugation oriented at ninety degrees to each other in successive layers. The Lithobrazed solder, which comes in the form of thin circular rods, is introduced into the valleys of the corrugations in each successive layer, so that when the sample is heated up in the furnace, the solder melts and flows down, accumulating around the points of contact between successive layers. The laminate wire mesh assembly for fabrication of the sample is supported within a wire mesh box (named support) with a weight plate on top inside a steel cup. The steel cup is placed inside the outermost container, which is a rectangular hollow box machined from steel. The top plate of the outermost container has a circular hole in it for introduction of the Argon gas as shown in the figure. Some pure Titanium powder is kept on top of the sample supported by a fine wire mesh to ensure removal of all oxygen from the container by oxidation. At elevated processing temperature, any oxygen in the inner atmosphere of the container that is driven upwards by the incoming argon will react with the pure Titanium powder and be rendered harmless. The sample is separated from the base of the steel cup by a layer of Nicrobrazed stop-off. The Nicrobrazed green stop-off (manufactured by Wall Colmonoy Corp., Madison Heights, MI, USA) was used to avoid the sample sticking to the contact surface at the high furnace temperature. The infiltration of atmospheric air into the main container is further prevented by one or two layers of ceramic paper covering the steel cup from top [20]. The ceramic paper, made from alumina ( $Al_2O_3$ ) fibers, can endure a very high temperature and prevents external air from entering the box. Ceramic paper is commonly used as combustion chamber liners, basket and tray linings, thermal and electrical insulation and in brazing/heat-treatment operations.

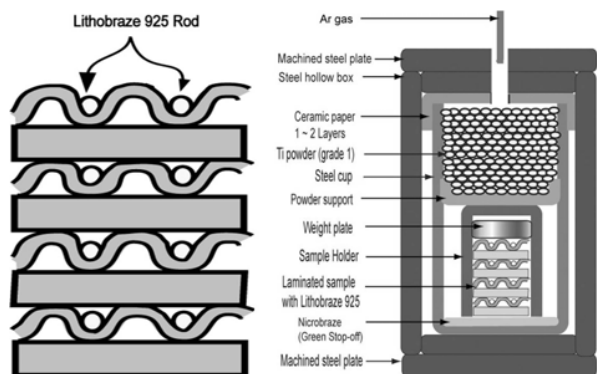


Fig. 1 Lamination assembly and fabrication chamber for high temperature Argon brazing

The steps involved in the Lithobrazed technique used for manufacturing the 304SST specimens are illustrated in Figure 2. They consist of (a) applying Nicrobrazed to the bottom of the steel cup and introducing the corrugated mesh layers into it, (b) placing the weight plate on top of the sample, (c) placing the mesh support to cover the sample, (d) placing the circular mesh sheet on top of the mesh support to hold the Titanium powder, (e) pouring the fine Ti powder on top to protect from oxidation, and (f) heating. Steps (a) through (f) comprised a complex

procedure which is followed by introducing the whole fabrication chamber into the furnace, connecting the argon feed and heating the furnace to the required temperature level. The heating of the furnace to a temperature at  $925^{\circ}C$  took about five to six hours. The temperature was maintained at this maximum level for about 25 minutes before cooling began.

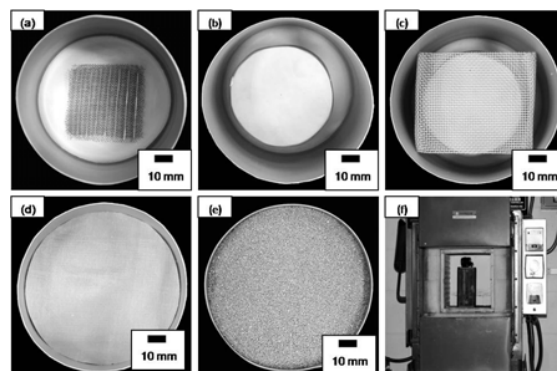


Fig. 2 Steps involved in Lithobrazed fabrication of CWML

The main advantage of the Lithobrazed fabrication technique described above is that it provides very effective protection from oxidation of the sample and hence ensures good bonding. The Lithobrazed solder materials melts into a liquid with low viscosity at the high temperature employed so that it can easily flow through the small mesh opening spaces. Hence this technique could be used to make CWML laminates with opening widths as small as 0.15 mm. Another advantage was that the depth of the containers and the easy downward feeding of the molten Lithobrazed by gravity allowed the manufacture of thick laminates with as many as 20 layers. The main disadvantages of the Lithobrazed technique were the complexity of the fabrication method, the long preparation and heating time involved, and the need for many accessories and consumables, some of which, e.g., the pure Ti powder used for oxidation protection, were quite expensive.

### C. Fabrication of CWML by Eutectic Soldering Technique

The brazing material employed for the Eutectic soldering was EutecticRod157PA which contained 95% Tin and 5% Silver (95Sn-5Ag). Eutectic Tin solder alloys are generally used for joining and repair of stainless steel. Its features are high fluidity, full joint penetration, very low heat input, excellent corrosion resistance and ease of use. The melting range of the Eutectic Tin alloys is from  $220$  to  $240^{\circ}C$  ( $428$ - $464^{\circ}F$ ). The furnace temperature employed for soldering in this study was  $225^{\circ}C$  ( $446^{\circ}F$ ). The shear strength of this solder alloy is 35-45 MPa (DIN 8526 standard test value). The Eutectic Tin-Silver alloy is often employed for the manufacture of medical and surgical equipment due to its biocompatibility [21].

The fabrication of the CWML samples using the Eutectic Sn-Ag soldering process is a much simpler process compared to the Lithobrazed technique. The samples were prepared by arranging the corrugated layers in the predetermined sequence required for the laminates. The solder material, EutecticRod

157PA, which comes in the form of a paste and includes a flux, was applied to the joints of the samples manually with a fine brush.

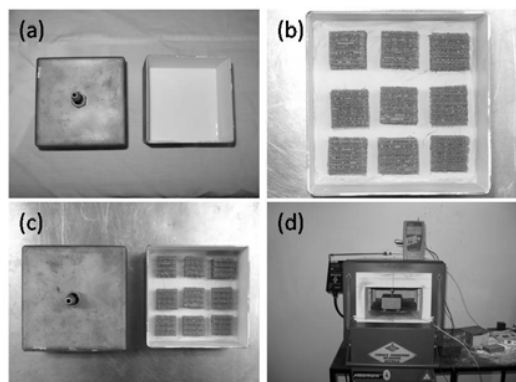


Fig. 3 Steps involved in Eutectic fabrication of CWML

Multiple samples were then placed in a steel container whose inner walls are painted with R104 (stop-off) solution to prevent adhesion. The Eutectic R104 is a protective shielding compound, often used for shielding metal surfaces during powder metal spraying. Unwanted metal particles adhering to

TABLE II  
CWML SAMPLE DATA

Specimen		Mesh per		Laminate sample data				
Steel type	Number of layers	Designation	(inch)	(mm)	Volume (mm <sup>3</sup> )	Weight (g)	Density, $\rho^*$ (g/cm <sup>3</sup> )	$\rho^*/\rho_s$
304SST	10	A	24	0.945	22292.5	9.00	0.404	0.05
	10	B	26	1.024	28468.0	10.2	0.358	0.045
	20	C	26	1.024	44261.7	16.6	0.375	0.047
	20	D	28	1.102	93149.5	51.0	0.548	0.068
	20	E	32	1.26	97585.6	30.0	0.307	0.038
	20	F	40	1.575	73331.4	49.5	0.675	0.084
	20	G	50	1.969	85834.6	61.2	0.713	0.089
	20	H	80	3.150	79446.9	57.7	0.726	0.091
316SST		K1-1	27	1.063	1890.0	0.4	0.212	0.026
		K1-2	27	1.063	1731.2	0.5	0.269	0.034
		K1-3	27	1.063	1940.4	0.5	0.249	0.031
	1	K1-4	27	1.063	1696.5	0.4	0.247	0.031
		K1-5	27	1.063	1957.1	0.5	0.232	0.029
		K1-6	27	1.063	1658.1	0.4	0.269	0.034
		K1-7	27	1.063	1735.5	0.4	0.252	0.032
		K2-1	27	1.063	3554.2	0.9	0.248	0.031
	2	K2-2	27	1.063	3131.7	1.0	0.316	0.04
		K2-3	27	1.063	2883.4	1.0	0.333	0.042
		K4-1	27	1.063	7147.6	1.9	0.271	0.034
		K4-2	27	1.063	6903.3	2.1	0.301	0.038
		K4-3	27	1.063	7346.6	2.4	0.326	0.041
	4	K4-4	27	1.063	7363.5	2.0	0.266	0.033
	K4-5	27	1.063	6624.8	2.0	0.3	0.038	
	K4-6	27	1.063	6858.1	2.2	0.323	0.04	
	K4-7	27	1.063	6566.2	2.4	0.369	0.046	

the compound are removed when the compound is washed or brushed off, leaving clean, unsprayed surfaces [21]. The container with the samples is then tightly closed and placed inside the furnace for heating. Argon gas is continuously supplied into the furnace during the fabrication process to provide an inert atmosphere and prevent oxidation of the samples. Note that at the processing temperature of 225<sup>o</sup>C employed for the Sn-Ag Eutectic solder alloy, the susceptibility of the steel to undergo oxidation is much lower and the inert argon atmosphere is sufficient to ensure that it is prevented. These steps are illustrated in Figure 3. Figure 3(a) shows the samples inside the steel container; Figure 3(b) shows the container box with the lid open and Figure 3(c) shows the top surface of the lid with the hole and connector for the entry of the argon gas into the container. Figure 3(d) shows a schematic of the container with the sample inside the furnace, with the argon supplied from the top.

The heating of the furnace to the required temperature took about 30 to 50 minutes after which the temperature was maintained at a 225<sup>o</sup>C for 30 min., prior to switching the heat off for cooling. The supply of Argon gas was maintained until the furnace returned to room temperature and the samples were ready to be removed. After removal from the furnace, the bonded samples were cleaned by distilled water using a brush to remove the flux. Finally, the washed samples were cleaned again using 99.9% purified methanol for 10 minutes. For the next round of preparation, the steel rectangular box was cleaned by a glass-blaster and then the surface inside the box was again painted with the R104 stop-off material. The main advantages of the Eutectic manufacturing technique were the savings in cost and time, the energy savings and the reduced safety risk due to the lower furnace temperature. The main disadvantages, compared to the Lithobrazing technique, are the need to apply the solder material to the joints of the sample manually and the fact that due to the higher viscosity of the molten Eutectic solder, it is difficult to fabricate laminates with finer mesh. Fig.4 shows typical samples fabricated with the Lithobrazing and Eutectic soldering methods.

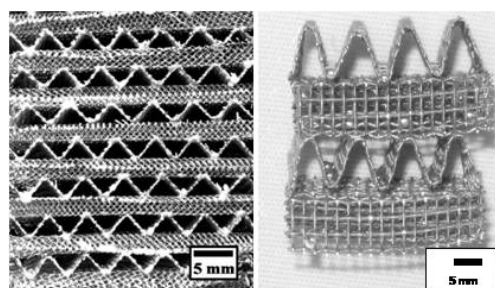


Fig. 4 CWML samples (left: 304SST fabricated with Lithobrazing, right: 316SST fabricated with Eutectic soldering)

### III. MECHANICAL BEHAVIOR

#### A. Relative Density of CWML Laminates

The properties of the corrugated wire mesh laminate samples

fabricated using the two bonding techniques described above are listed in Table II. Eight samples of CWML were constructed with 304SST each with a different grade mesh, as mentioned before. Two of these eight samples had 10 layers of corrugated mesh while the other six had 20 layers. The 304SST CWML samples are labeled A to H. Seven of the 316SST samples were single layer corrugated wire meshes, these are labeled K1-1 to K1-7. Three 316SST laminates were fabricated with two layers of corrugated meshes (K2-1 to K2-3) and a further seven with four layers of corrugated wire mesh (K4-1 to K4-7). The wire mesh properties as well as laminate data, consisting of volume, weight, and density, of all the CWML samples fabricated are also listed. The last column of Table II lists the relative density, which is the ratio of the density of the laminate to the density of the steel wire material. It may be noted that the effective density of the CWML is much lower than the density of steel, with the 304SST samples, constructed with denser meshes, being about 10 to 20 times lighter than steel and the 316SST samples 20 to 40 times lighter than steel. The relative densities of CWML laminates are four to five times smaller than the wire meshes with which they are made; this is the effect of the corrugation, which increases the volume occupied by each layer of the mesh. Considering the single layer, double layer and the four layer CWML constructed with the 316SST in particular, since they are all constructed with the same wire mesh (grade designated K) and the corrugation is the same, one would expect their relative densities to be the same. However, it is seen that the average densities of the 2 layer laminates and the 4 laminates are higher than those of the single layer corrugated meshes. The average density of the seven single layer samples is  $0.25 \text{ g/cm}^3$ , while those of the 2 layer and the 4 layer laminates are  $0.30$  and  $0.31 \text{ g/cm}^3$ , respectively. The increase in relative density with increasing layers of the laminate can be attributed to the increase in mass due to the addition of the solder in the joints.

### B. Compressive Behavior of CWML Laminates

The laminates fabricated with 316SST using the Eutectic soldering technique were tested in uniaxial transverse compression. A Universal testing machine (Shimadzu Autograph AG-10TA, Japan) was used for the compression tests. The samples were loaded at a controlled displacement rate of 50mm/min. Typical compressive behavior of the one layer sample is illustrated with photographs taken at 10% increments of the axial strain in Figure 5.

The typical engineering stress vs. strain plots of single layer, two layer and four layer CWML laminates are shown in Figure 6. The engineering stress plotted on the Y axis is the axial transverse pressure applied to the laminates, given by the applied load divided by the plan form cross section area of the laminate. The engineering strain on the X axis is the change in height over the original height of the laminate. It can be seen that the behavior of the CWML laminates is similar to the compressive behavior of foam and other open and closed cell structures, with an initial quasi-linear elastic phase topped by yielding (identified with the peak stress value), which is

followed by a plateau ending in strain hardening region corresponding to densification of the individual layers.

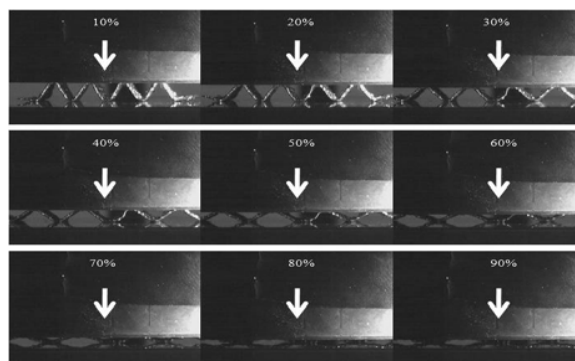


Fig. 5 Compressive behavior of Single Layer 316SST sample with increasing load (photographs taken at 10% strain increments)

The initial stiffness of CWML, given by the gradient of the elastic region, is almost identical for the one layer, two layer and the four layer laminates, while the peak stress shows only a small variation in magnitude. However, the behavior of the three types of laminates is markedly different in the post yield region. The one layer laminate shows a strain softening regime immediately after yielding before leveling to a plateau at a strain of about 25%. The plateau extends to about 75% strain level before it enters the strain hardening phase due to densification of the material. With increasing numbers of layers, the strain softening region and the plateau become smaller and smaller, with the four layer laminate almost directly entering the strain hardening phase after yield. The ultimate strains of the samples fall between 0.8 and 1.0.

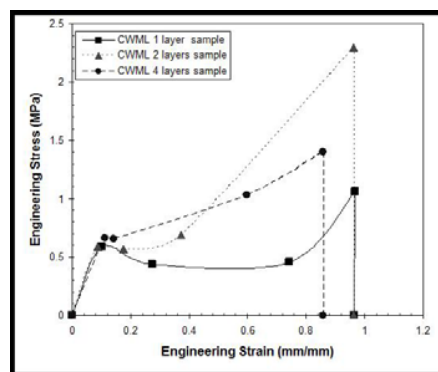


Fig. 6 Compressive Stress Strain behavior of 1, 2 and 4 layer CWML samples

Figures 7 and 8 respectively show the variation of the yield stress and the initial effective laminate stiffness (gradient of the linear segment of the stress vs. strain plot) with increasing number of layers in the CWML. The yield strength shows a small increase with increasing number of layers. The change in effective stiffness is quite significant from the single layer to the two layer geometry, but appears to level out after that. This is similar to the variation of the relative densities of the CWML with increasing number of layers described previously and can be attributed to the same cause. It is believed that the reason for



the small increase in the stiffness and the peak load carried by the laminates is the addition of the bonding material at the joints which increases their stiffness making the wire segments connecting them more rigid. The secondary effect of the addition of the bonding material on the stiffness and the strength is largest when the bonding is first introduced in the two layer laminate, having smaller increments with further increase in layers. The additional stiffness provided by the bonds at the joints may also explain the increasing strain hardening behavior of the laminates with increasing number of layers. In the single layer laminates once the corrugations start flattening out after yielding at the vertices, there is no additional resistance and hence no increment in load is required for the deflection to keep increasing until the corrugation is virtually flattened out and enters the densification phase. In the case of multilayer laminates, the bonds between the adjacent layers constrain the corrugations from flattening out easily (noting that the corrugations runs in perpendicular directions in adjacent layers), requiring an increase in load for increasing displacement.

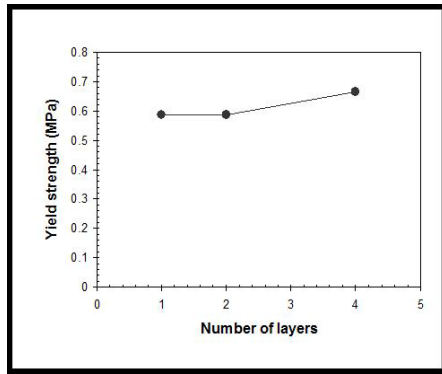


Fig. 7 Variation of Yield Strength with number of layers in CWML laminate

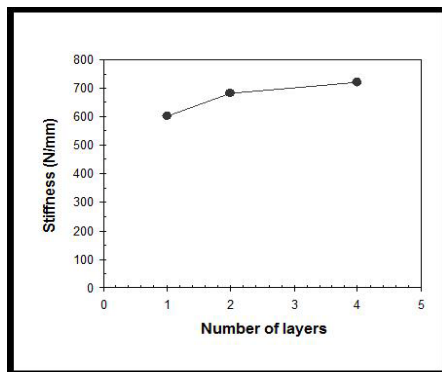


Fig. 8 Variation of transverse stiffness with number of layers in CWML laminate

### C. Comparison with Gibson-Ashby Theory

According to Gibson-Ashby, cellular foam and open celled cellular structures show a stress strain behavior consisting of three distinct phases: a linear elastic region, plastic yielding followed by a long plateau and a sharp stress growth due to densification [22]. The behavior of the CWML laminates

correspond to this classic description, as seen in Figure 6, except that, with increasing number of layers, the plateau becomes smaller and smaller and stress hardening due to densification appears to occur earlier. Ashby Gibson also showed that there is an exponential relation between the relative load capacity of the open cell structure, and the relative density of the structure [22]. They have also shown that this applies to a variety of open and closed cell structures, including polymeric foams and cancellous bone; with some variations in the value of the exponent and the linear coefficient with varying material properties. The applicability of this theory to CWML was examined by considering the variation of the yield stress, extracted from the test data, with the relative densities of the CWML samples and comparing it with the Gibson-Ashby formula. Gibson and Ashby have shown that the “yield stress” or the stress at which plastic hinge forms in the structure limiting the load capacity of the open cell structure is effectively equal to the value of the true stress at a true strain value of 25% [22]; the same terminology and definition was employed in this study to determine the yield stress values for comparison stress. Figure 9 shows the variation of the yield stress for the CWML samples tested (corresponding to the true stress level at a strain value of 0.25) with the relative density of the samples, plotted on a Log-Log scale. Also plotted in the figure are straight lines representing the Gibson-Ashby formula for a value of 1.5 for the exponent, applicable to metallic foams, for values of the linear coefficient  $C$  equal to 0.1, 0.3 and 0.5. The values of the 304SST laminates, represented by the filled triangles, lie closest to the line with  $C=0.1$ , but show a wide variation or large amount of scatter, possibly due to the fact that these samples were all manufactured with different grades of meshes. The data from the CWML samples made of 316SST, all manufactured from the same type of mesh, all bunched closer together, with the single layer data, represented by circles filled with black at the bottom, the data of the 2 layer samples, represented by the filled squares at the top and the data from the four layer samples, circles filled in grey, in between. All the 316SST data points are centered along the Gibson-Ashby line with  $C=0.3$ .

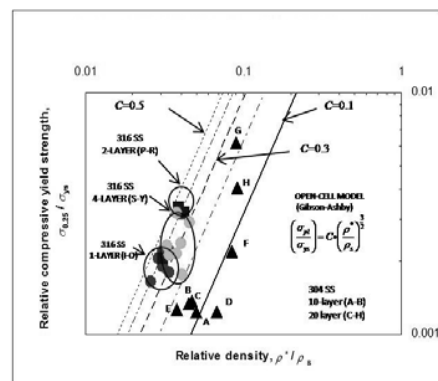


Fig. 9 Variation of Yield Stress with relative Density compared to Ashby Gibson theory

### IV. CONCLUSION

Two different manufacturing processes for the fabrication of

corrugated wire laminates were described. The first one utilizes Lithobraz, a brazing agent with Silver, Copper and Lithium, which has a melting temperature over 760°C, and hence requires a rather complex set-up for processing and to prevent oxidation of the sample during the brazing process. This method is thus time consuming, labor intensive and costly, but offers the advantage that it can be used to bond finer meshes and laminates with a large number of layers. The second manufacturing technique uses a Eutectic Sn-Ag soldering alloy with a melting temperature of 225°C, making it a simple, easy and cost effective method of fabricating CWMLs. One of the main disadvantages of this method is that the solder alloy has to be manually applied to each joint in the laminate, limiting its application to laminates with only a small number of layers; another is that, due to the higher viscosity of the molten solder, it does not easy flow out of the samples, thus limiting the fineness of the mesh to which it can be applied. The effective density of the CWML structures is 10 to 40 times lower than that of the base material used for its manufacture.

The CWML samples were subjected to uniaxial compression and it was found that in general the behavior of corrugated wire mesh laminate is similar to that of open celled foam. The initial axial stiffness and the peak stress of the laminates do not vary significantly with increasing corrugated layers. The variation of the plastic stress with relative density appears to be in reasonable agreement to the theory developed by Gibson and Ashby for open celled structures for a value of 0.3 for the linear coefficient.

#### ACKNOWLEDGMENT

The first author Jeongho Choi thanks Prof. D. J. Sypeck of Embry-Riddle Aeronautical University at Daytona Beach, Florida, USA, for raising his interest and knowledge on this topic and for providing guidance during his post graduate degree program at Embry-Riddle Aeronautical University.

#### REFERENCES

- [1] Ho-Sung Lee, Jong-Hoon Yoon, Yeong-Moo Yi, *Oxidation behavior of Titanium alloy under diffusion bonding*, *Thermochimica Acta* 455, 2007, pp.105-108
- [2] TWI, UK (<http://www.twi.co.uk/content/kssbd003.html>)
- [3] Thomas Studnitzky, Rainer Schmid-fetzer., *Phase formation and diffusion soldering in Pt/In, Pd/In, and Zr/Sn thin-film systems*, *Journal of electronic materials*, vol.32, No.2., 2003, pp. 70-80
- [4] G.He, M.Hagiwara, *Ti alloy design strategy for biomedical applications*, *Materials Science and Engineering C*, 26, 2006, pp. 14-19
- [5] G.He, M.Hagiwara, *Ti-Cu-Ni (Fe,Cr,Co)-Sn-Ta(Nb) alloys with potential for biomedical applications*, *Materials Transactions*, vol.45, No.4, 2004, pp.1120-1123
- [6] G.A. Lopez, *Kinetic behaviour of diffusion-soldered Ni/Al/Ni interconnections*, *Materials Chemistry and Physics* 78, 2002, pp.459-463
- [7] M. J. Kim, R. W. Carpenter, M. J. Cox, J. Xu, *Controlled planar interface synthesis by ultrahigh vacuum diffusion bonding/deposition*, *J.Mater.Res.*, Vol.15, No.4, Apr 2000, pp.1008-1016
- [8] M.Eroglu, T.I.Khan, N.Orhan, *Diffusion bonding between Ti-6Al-4V alloy and microduplex stainless steel with copper interlayer*, *Material Science and Technology*, vol.18, Jan 2002, pp.68-72
- [9] Carles L. Bauer, *Metal-joining methods*, *Annu.Rev.Mater.Sci.*, 6, 1976, pp. 361-387
- [10] E.Lugscheider, K.Bobzin, M.K.Lake, *Deposition of solder for micro-joining on M.E.M.S. components by means of magnetron sputtering*, *Surface and Coatings Technology*, 142-144, 2001, pp.813-816
- [11] W.D.MacDonald, T.W.Eagar, *Transient liquid phase bonding*, *Annu.Rev.Mater.Sci.* 1992, 22:23-46
- [12] Mitsuo Niinomi, *Recent research and development in Titanium alloys for biomedical applications and healthcare goods*, *Science and Technology of Advanced Materials* 4, 2003, pp. 445-454
- [13] E.Lugscheider, S.Ferrara, H.Janssen, A.Reimann, B.Wildpanner, *Progress and developments in the field of materials for transient liquid phase bonding and active soldering process*, *Micro system technologies* 10, 2004, pp.233-236
- [14] C. Kanchanomai and Y. Mutoh, *Effect of temperature on isothermal low cycle fatigue properties of Sn-Ag eutectic solder*, *Materials Science and Engineering A* 381, 2004, pp. 113-120
- [15] John Chisholm, *Method of making a crimped wire mesh heat exchanger/sink*, U.S.Patent, No. 4,843,693, July 4, 1989
- [16] David Sypeck, Hayen N.G. Wadley, *Multifunctional periodic cellular solids and the method of making same*, U.S. Patent, No.US2004/0154252A1, Aug.12, 2004
- [17] D.J. Sypeck, H.N.G. Wadley, *Multifunctional microtruss laminates: Textile synthesis and properties*, *J. Mater. Res*, Vol. 16, No. 3, March 2001, pp 890-897
- [18] M.F. Ashby, A.Evans, N.A.Fleck, L.J.Gibson, J.W.Hutchinson, H.N.G.Wadly, *Metal foams-a design guide*, Butterworth-Heinemann, Elsevier, 2000
- [19] Lucas-Milhaupt, Inc., *VTG/High purity silver, gold, palladium*, accessed May 20, 2004. ([http://www.lucasmilhaupt.com/htmldocs/brazing\\_products/brazing\\_fill\\_er\\_metals/high\\_purity.html](http://www.lucasmilhaupt.com/htmldocs/brazing_products/brazing_fill_er_metals/high_purity.html))
- [20] Choi, J.H., *Fabrication and compressive yield strength of open cell corrugated cellular solids*, master thesis, Embry-Riddle Aeronautical University, Daytona Beach, Florida, U.S.A., 2005
- [21] Eutectic Australia Pty Ltd, *Product data guide*, 2006
- [22] L. J. Gibson, M. F. Ashby (1997). *Cellular solids Structure and Properties*, 2nd ed., United Kingdom : Cambridge University Press, Cambridge
- [23] Ashby. M.F., *Materials Selection in Mechanical Design*, Pergamon Press, UK, 1992
- [24] Fleck, N.A. and Khang, K.J. and Ashby, M.F., *The cyclic properties of engineering materials*, *Acta Metallurgica et Materialia*, 42 (2), 1994, pp. 365-381. ISSN 0956-7151
- [25] Mills, N.J. and Gilchrist, A., *The Effectiveness of Foams in Bicycle and Motorcycle Helmets*, *Accid. Anal. and Preview*, 23, pp153-163, 1991